Journal of Theoretical Biology 259 (2009) 760–769

Contents lists available at ScienceDirect

Journal of Theoretical Biology

journal homepage: www.elsevier.com/locate/yjtbi

Boolean network-based analysis of the apoptosis network: Irreversible apoptosis and stable surviving

Zhongxing Mai, Haiyan Liu *

School of Life Sciences and Hefei National Laboratory for Physical Sciences at the Microscale, University of Science and Technology of China, Hefei, Anhui 230027, PR China

ARTICLE INFO

Article history:
Received 25 November 2008
Received in revised form
19 April 2009
Accepted 21 April 2009
Available online 5 May 2009

Keywords:
Signal transduction network
Irreversibility
Stability
Feedback loops
Lethal initial states
Robustness

ABSTRACT

To understand the design principles of the molecular interaction network associated with the irreversibility of cell apoptosis and the stability of cell surviving, we constructed a Boolean network integrating both the intrinsic and extrinsic pro-apoptotic pathways with pro-survival signal transduction pathways. We performed statistical analyses of the dependences of cell fate on initial states and on input signals. The analyses reproduced the well-known pro- and anti-apoptotic effects of key external signals and network components. We found that the external GF signal by itself did not change the apoptotic ratio from randomly chosen initial states when there is no external TNF signal, but can significantly offset apoptosis induced by the TNF signal. While a complete model produces the expected irreversibility of the apoptosis process, alternative models missing one or more of four selected inter-component connections indicate that the feedback loops directly involving the caspase 3 are essential for maintaining irreversibility of apoptosis. The feedback loops involving P53 showed compensating effects when those involving caspase 3 have been removed. The GF signal significantly increases the stability of the surviving states of the network. The apoptosis network seems to use different modules by design to control the irreversibility of the apoptosis process and the stability of the surviving states. Such a design may accommodate the needed plasticity for the network to adapt to different cellular environments: depending on the strength of external pro-surviving signals, apoptosis can be induced either easily or difficultly by pro-apoptotic signal of varying strengths, but proceed with invariable irreversibility.

© 2009 Elsevier Ltd. All rights reserved.

1. Introduction

Apoptosis or programmed cell death has been subjected to extensive experimental studies for more than two decades. In the apoptosis process, a range of cellular signals are integrated by a complex molecular network (Falschlehner et al., 2007; Henson and Gibson, 2006). This network as a whole, not the status of individual signaling molecules controls when a cell can (or should) no longer survive and enter programmed death irreversibly (Janes et al., 2005). To understand how the network operates, it is necessary not only to study what are its composing components or what molecular interactions exist between the components, but also to analyze the network as a whole or at the systems level to identify which of its properties are essential for biological functions, and how these properties emerge from the specific way by which the interacting components are organized into an integrated system. In the latter regard, computer models formulating the various molecular components and their interactions can in many aspects complement experimental studies. One main advantage of using computer simulations for systems level analysis is that components or interactions can be systematically varied in silico, either individually or jointly, to probe their roles in any general or specific cellular contexts (Stelling, 2004; Wolkenhauer, 2002).

Depending on the states of its components and the signals it receives, the outcome of the apoptosis network can be either surviving or apoptosis. Essential systems level properties of the network should include the robust stability of the surviving state as well as the irreversibility of the survival to apoptotic transition. The former property means that apoptosis can be triggered only by some definite cellular signals, but not by spontaneous fluctuations in the states of individual molecular components. The latter property means that apoptosis, once started, cannot be abolished either by withdrawing of the triggering signals or by spontaneous fluctuations.

How multi-stability and irreversibility generally arise in cellular networks and what their biological implications are have been analyzed theoretically and in some cases demonstrated experimentally (Ferrell, 2002; Ferrell and Xiong, 2001). In these studies, irreversibility and multi-stability have often been

* Corresponding author. Tel.: +86 551 3607451.
E-mail address: hyliu@ustc.edu.cn (H. Liu).

0022-5193/$ - see front matter © 2009 Elsevier Ltd. All rights reserved.
doi:10.1016/j.jtbi.2009.04.024

attributed to nonlinear dynamics associated with feedback loops in the respective networks.

As for the apoptosis network in particular, a number of computer modeling studies based on ordinary differential equations (ODE) have been reported (Bentele et al., 2004; Albeck et al., 2008; Rehm et al., 2006; Bagci et al., 2006; Eissing et al., 2004; Legewie et al., 2006). These ODE models are based on detailed knowledge or assumptions of kinetics parameters associated with all molecular processes considered in the respective models, and provide detailed dynamics of these processes. Thus an advantage of ODE models is that they can not only be used for theoretical analyses (Bagci et al., 2006; Eissing et al., 2004; Legewie et al., 2006), but also be calibrated based on and then tested against quantitative experimental measurements when such measurements are available (Albeck et al., 2008; Rehm et al., 2006). However, most previous ODE models have focused on limited parts of the apoptosis network. To obtain a more complete picture, it is of interest to investigate more extensive networks, especially those involving the interactions of apoptotic pathways with surviving pathways such as the growth factor (GF) pathway. As more molecular components are included, it becomes increasingly challenging to develop mutually compatible ODEs to cover all the different types of molecular processes. Moreover, in the higher-dimensional continuous state space of the ODE framework, it is difficult to formulate and extract systems properties from the complex dynamics. It is also difficult to perform systematic explorations in the model space, kinetic parameter space as well as in the initial condition space.

Boolean network (BN) is an alternative way to model complex cellular networks. A BN is a qualitative mathematical model composed of nodes having discrete states and rules governing the temporal evolution of the states. Since introduced by Kauffman in late 1960s (Kauffman, 1969), BN has been used to model gene regulatory networks and signaling pathways (Huang and Ingber, 2000; Li et al., 2004). Although BN does not model dynamics in terms of continuous variables, it has been argued that BN may provide good approximations to a variety of nonlinear behaviors of biological systems (Amaral et al., 2004). The state space of BN is discrete by definition, and is thus more accessible to statistical analyses. Such analyses readily enable the formulation and extraction of systems level properties for relatively large networks of higher dimensional variable spaces. BN can also afford extensive explorations in the model space and the initial condition space in such systems.

In this work, we construct a 40-node Boolean model of the cellular apoptosis network to analyze its systems properties and how they can be linked to specific structural features of the network. Because of the simplicity of BN, we are able to consider a relatively complete set of known molecular processes, including both anti-apoptosis (or pro-survival) and pro-apoptosis pathways, and the integration of intrinsic and extrinsic signals. One major purpose of our study is to understand the emergence of systems properties. These include the stability of the surviving states and the irreversibility of the apoptotic process. Through extensive analyses of the state space, we try to identify key network components that lead to these properties. In silico experiments are performed with a large number of random initial states at different combinations of input cellular signals. Critical pro-survival and pro-apoptotic nodes are identified based on statistical correlations between initial states and final outcomes. Irreversibility of the apoptotic process is characterized using time-dependent input signals. Stability of the surviving states is analyzed based on perturbations in the state space. The roles of specific feedback structures in the network are investigated using simulated knockout experiments.

2. Materials and methods

2.1. Structure of the model

Our BN model (Fig. 1) includes 37 internal nodes representing states of signaling molecules, 2 input nodes representing extracellular signals, and 1 output node corresponding to the DNA damage event. The nodes are interconnected, connections corresponding to a set of rules defining how the states of each node evolve in time depending on the states of other nodes (see below). This model is based on extensive surveys of literature as well as on expert-curated databases, especially the reactome database (http://www.reactome.org). Given the complexity of the real networks in cells and our incomplete current knowledge of them, our model is necessarily approximate. The main considerations in choosing nodes and connections are to include as complete as possible known connections that may integrate major extracellular signals determining the survival or apoptosis of cells. Generally accepted major molecular players such as p53 and NFκB are also included. Different molecules may be represented by a single node if they have been reported to play the same or similar roles (e.g., proteins in the same family and of not clearly distinguishable functions, such as the different types of GF signals or different IAPs). More details of the network structure are described below.

2.1.1. Modeling the extrinsic pro-apoptotic signals

The extrinsic apoptotic pathway involves the activation of the tumor necrosis factor (TNF) family of receptors (TNFRs), represented by TNFR1 and TNFR2 in our model. We use TNF receptor-associated death domain protein (TRADD) to represent the direct downstream targets of TNFR1 (Wang et al., 1999). The major pro-apoptosis effects of these receptors are modeled by the activation of Fas-associated death domain protein (FADD), which in turn leads to the activation of caspase-8 (Morgan et al., 2001). The effects of the extrinsic pro-apoptotic signals on the intrinsic apoptotic pathways are modeled through the activation of receptor-interacting protein (RIP), which then induces p53 activation through a mitogen-activated protein kinase cascade (represented by MEKK-1, JNKK and JNK in the model) (Kelliher et al., 1998; Lin et al., 2000).

2.1.2. Modeling the pro-survival effects of extrinsic TNF signals

The pro-survival effects of these receptors are modeled first as the activation of caspase-8 inhibitory proteins (represented as the cellular form of FLICE-inhibitory protein (cFLIP) in our model) by TNF receptor-associated factors (TRAF), and second as the TNFR-mediated activation of NFκB through the removal of the inhibitor of NFκB protein (IkB) by the activated IkB kinase (IKK) complex. In our model, extrinsic TNF signals have both inhibitory (through TNFR1, RIP and then TRAF2) and activating (through TNFR2 and then TRAF2) effects on NFκB (Kelliher et al., 1998; Lin et al., 2000; Muppidi et al., 2004; Shu et al., 1996; Wu et al., 2005). NFκB exerts negative feedback regulation on its own inducing pathway via activating A20 and IkB (De Valck et al., 1997; Ferran et al., 1998).

2.1.3. Modeling the pro-survival effects of extrinsic growth factor signals

The transduction of extrinsic pro-survival signals is modeled through the growth factor receptors (GFR) and the Akt/PKB protein kinases. Activated GFR activates phosphatidylinositol 3-kinase (PI3K), which produces phosphatidylinositol trisphosphate (PIP3) from PIP2. PIP3 activates Akt (Song et al., 2005). In our model the pro-survival effects of Akt are achieved through its

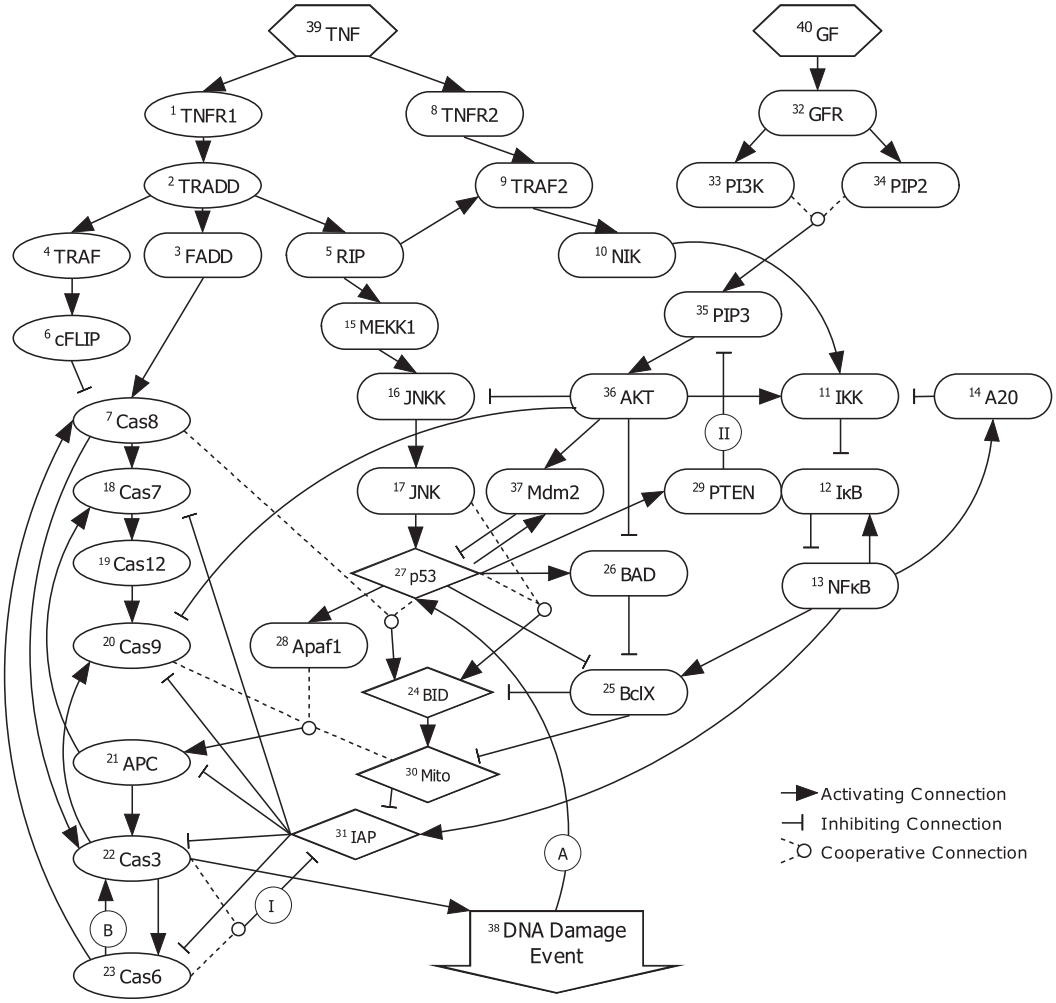

Fig. 1. The Boolean network model. The integer ID of each node is at the top left corner of the label. Each edge corresponds to inhibiting or activating connections. The cycled labels A, B, I and II indicate connections removed in the knockout experiments. Reversing the states of nodes represented as cycles may result in survival→apoptosis transitions when GF is OFF. Nodes as diamond boxes may results in survival→apoptosis transitions when GF is ON.

inhibitory action on the caspase machinery (on caspase 9), on the activation of p53 (on the TNFR mediated MAPK kinase cascade and through murine double minute 2 protein (Mdm2)), as well as on the intrinsic inventory of pro-apoptotic Bcl2-like molecules (on Bcl-2-associated death promoter (BAD)).

2.1.4. *Modeling the intrinsic apoptotic pathways*

The intrinsic apoptotic pathways are modeled by including the anti-apoptotic (BclX) and pro-apoptotic (BAD) Bcl2 family of proteins (Shimizu et al., 1999). BAD received activating or pro-apoptotic signals from p53 and inhibitory or pro-survival signals from Akt, and achieves pro-apoptotic effects via inhibitory effects on BclX. BclX prevents the release of apoptotic signals from mitochondrion (mito) which promotes the formation of the apoptosome complex (APC). The latter needs also apoptotic protease activating factor 1 (Apaf1) and activated caspase 9. Pro-apoptotic molecules released by mitochondrion (e.g., Smac) also neutralize the inhibitors of apoptosis (IAP). The node Mito represents the complex but still unclear regulations of the releasing of cytochrome c and Smac by other molecules.

2.1.5. *Modeling connections at p53*

We model the central regulator p53 as receives input from both the extrinsic pro-apoptotic (mediated by TNFR) and pro-survival signals (via Akt) as well as the intrinsic apoptosis signals, and generates pro-apoptotic output via Bad, Apaf1, and Bid (Haupt et al., 2003; Kim et al., 2005; Yu and Zhang, 2005).

2.1.6. *Modeling the caspase machinery*

Caspase 3 is the terminal promoter for apoptosis in the model, which not only receives the extrinsic and intrinsic apoptotic input signals via caspase 8 and APC, respectively, but also receives the pro-survival signals from Akt and IAPs. The caspase machinery is modeled as the main activation cascade from caspase 8 to caspase 3, the activation of caspase 7 by caspase 8 or APC which then leads to the activation of caspase 9, the activation of caspase 3 by caspase 9 involving APC, as well as the three positive feed backs from caspase 6 to caspase 3, from caspase 6 to caspase 8 and from caspase 3 to caspase 9 (Mak and Yeh, 2002; Philchenkov, 2004).

2.1.7. *Major connecting points and feedbacks between pathways*

Several major connecting points between extrinsic and intrinsic apoptotic pathways before the terminal caspase 3 are built into the model, including Bid that integrates signals from TNF (via caspase 8 and JNK) and p53 (Mak and Yeh, 2002; Yu and Zhang, 2005), and caspase 7 receiving inputs from caspase 8 and APC (Lowe et al., 2004; Philchenkov, 2004). The connections by which extrinsic pro-survival signals disrupt the apoptotic process

include those involving Akt as described above, and the activation of BclX and IAPs by NFκB (Bernal-Mizrachi et al., 2006; Deveraux and Reed, 1999). The GF pathway also receives negative feedback from p53 via PTEN which deposphorylates PIP3 (Okamura et al., 2006; Yan et al., 2006).

In some of our simulations, alternative models with selected connections knocked out from the complete model shown in Fig. 1 have been employed. The modifications involved in these models will be described in the results section.

2.2. Rules specifying the dynamics

Each node in the model can be in either the ON or the OFF state at a specific time step. Except for the TNF and GF nodes that correspond to external signals, each node receives inputs from one or several nodes (Fig. 1). There are two types of inputs: activating ones and inhibiting ones. The state of node i at the next time step $S_i(t+1)$ depends on its current state $S_i(t)$ as well as the relative magnitudes of the total activating input $A_i(t)$ and the total inhibiting input $H_i(t)$ it receives,

$$S_i(t+1)=\begin{cases}\text{OFF} & \text{if } A_i(t)<H_i(t),\\ \text{ON} & \text{if } A_i(t)>H_i(t), \quad \text{and}\\ S_i(t) & \text{if } A_i(t)=H_i(t).\end{cases} \tag{1}$$

The value of $A_i(t)$ ($H_i(t)$) is the summations of the contributions of all activating (inhibiting) input connections of node i. The contribution of each connection depends on the current states of the respective upstream nodes, and the dependence specified by one input connection rule. The input connections and the associated rules of each node are listed in supplementary table S1. To make the minimum hypothesis, most of the input rules have the same contribution of 1.0. A few rules are associated with arbitrarily larger values, to reflect the known or assumed dominating influences of the respective input connections (for example, the inhibiting input received by caspases from IAP is associated with a large value).

To mimic the threshold effects of caspase 3 in promoting apoptosis events, the evolution of the node "DNA Damage Event" does not follow Eq. (1) and is not first order in time. This node is always set to the OFF state unless the caspase 3 node has been in the ON state in previous two successive steps: only when both $S_{\text{Cas3}}(t-1)=\text{ON}$ and $S_{\text{Cas3}}(t)=\text{ON}$, $S_{\text{DNA Damage Event}}(t+1)=\text{ON}$, otherwise $S_{\text{DNA Damage Event}}(t+1)=\text{OFF}$.

2.3. Ending criteria and ending states of simulations

Time evolutions of the network are followed by simulations starting from different initial states. Each simulation run ends when either of the following two criteria was met. The first criterion is that the "DNA Damage Event" node has remained in the ON state for a predefined number of successive steps. This criterion as well as the corresponding ending states of the network is denoted as "apoptosis". The second criterion is that apoptosis has not taken place by the first criterion but a pre-specified maximum number of steps has been reached. The corresponding ending states are denoted as "survival" ones. To determine the parameters (numbers of steps) used in these criteria, we performed simulations with different parameters using a set of 10,000 individual initial states. Results listed in Table S2 show that it is sufficient to test for apoptosis in 20 successive steps and to set the maximum number of steps to 200. Using larger numbers for either criterion does not change the results (Table S2).

2.4. Apoptosis ratios

The initial states that end in "apoptosis" are noted as apoptotic initial states. For a given combination of input signals, we compute an apoptosis ratio as the fraction of apoptotic initial states in all randomly selected initial states,

$$\text{Apop\%}=\frac{\text{Number of apoptotic initial states}}{\text{Total number of initial states}}\times 100\%$$

2.5. Initial states

In this work, we aim at obtaining insights into the design principles of the apoptosis network in general. Specific cell types/cellular contexts are not considered. Thus we use unbiased random initial states. Initial states have been sampled at random: each of the 37 internal nodes has an independent probability of 0.5 to be in either the ON state or the OFF state. Simulation results using 10,000, 20,000, 50,000 and 100,000 initial states, respectively, are compared (Table S3), and 10,000 initial states have been found to be sufficient to produce good statistics. We would like to note that in a real experiment, only a small set of initial states would be possible, depending on contexts such as the specific cell type and the particular experimental setup. In most cases detailed knowledge of such dependences are unavailable. Using unbiased random initial states provide a statistical approach towards systems properties of a general apoptosis network in lack of such knowledge.

2.6. Input signal combinations

The temporal evolutions from each of the 10,000 initial states have been monitored with the following combinations of input signals: (1) with no input signals (both TNF and GF in OFF states); (2) with only the TNF signal ON; (3) with only the GF signal ON; and (4) with both the TNF and GF signal ON. Unless specified otherwise (see below), the states of the TNF and GF nodes do not change with time in a simulation.

2.7. Time-dependent or interrupted apoptotic signals

Interruptions of apoptotic signals in a simulation have been employed to investigate the irreversibility of the apoptosis process. Interruption is achieved by setting and maintaining a selected node in its OFF state. Interruptions of the external signal TNF or the internal mitochondria signal are introduced when the node "DNA Damage Event" has been in the ON state for 2 continuous steps, results compared with respective simulations without interruptions. The state of the "DNA Damage Event" node itself is not changed manually but follows the dynamics rules as described earlier.

2.8. Perturbations on the states of the internal nodes

The stability of the surviving ending states with respect to fluctuations in the states of the internal nodes has been investigated. Starting from an ending state, the states of internal nodes are systematically reversed (from ON to OFF or vise visa), either one by one (single-node perturbations) or two at a time (dual-node perturbations), to obtain various perturbed surviving states. Time evolution starting from each of the perturbed states has been followed until one of the previously described ending criterions has again been met.

3. Results and discussions

3.1. Initial states that lead to apoptosis independent of external signals

From the simulations, we found that some of the initial states (lethal initial states) led to "apoptosis" under all the four different input conditions. These states would not be observed in real experiments but provide basis to analyze the roles of individual network components. Table 1 lists the percentages of lethal initial states obtained using the complete model and two alternative models with selected connections removed. These include Model-B in which connection B (see Fig. 1, the positive feedback involving a pro-apoptosis node) has been removed and Model-I in which connection I (see also Fig. 1, the negative feedback involving a pro-survival node) has been deleted. The calculated ratios of lethal initial states do not depend on the set of initial states used, similar ratios of lethal initial states (47–48%) obtained from simulations with different sets of initial states (Table S3).

The state distributions of the internal nodes in the lethal initial states have been computed. Some of them are significantly biased towards either the ON or the OFF state. Table 1 lists those nodes whose probability to be in the ON state (p_i(ON)) in the set of lethal initial states deviates significantly from 0.5 (at confidence levels above 0.995 based on χ^2 tests).

Interestingly, some nodes showed up consistently in the above lists for both the complete model and the two alternative models. Among them, there are those corresponding to well-known pro-apoptotic components such as FADD, Cas8, IκB, Cas3, BID and mitochondria (Budihardjo et al., 1999; Ko et al., 2005; Li et al., 2005; Narita et al., 1998; Philchenkov, 2004; Sartorius et al., 2001), and those corresponding to anti-apoptotic components including cFLIP, NFκB, BclX and IAP (Bernal-Mizrachi et al., 2006; Deveraux and Reed, 1999; Deveraux et al., 1997; Gross et al., 1999; Shimizu et al., 1999).

The differences between the respective lists produced by the three models can be explained to a large extent by their different topologies. For example, in Model-B, one of the activating input connections into the primary apoptotic effector Cas3 was blocked. To induce apoptosis, compensating inputs from other activators are needed. These could potentially include APC and Cas8. As the assembling of APC is difficult in lack of the TNF signal, Cas8 becomes vital for later Cas3 activation in some lethal initial states. Thus in lethal initial states associated with Model-B, Cas8 has a significantly large p(ON) (0.65) while the Cas8-inhibitor cFLIP had a significantly small one (0.44). Similarly, in Model-I that misses one of the inhibiting input connections into the primary anti-apoptotic factor IAP, the mitochondria component that is the direct inhibitor of IAP has a significant high p(ON) (0.79).

It should be noticed that for over 40% of the internal nodes, their state distributions in the lethal or non-lethal initial states do not differ significantly. And for the remaining nodes the deviations of p(ON) from 0.5 in lethal initial states are not large. This suggests that the initial states of internal nodes as individual factors cannot dominate the final outcome of the network, in agreement with a previous data-driven modeling study (Janes et al., 2005).

3.2. The irreversibility of apoptosis and roles of feedback loops

Table 2 presents that in the complete model, Apop% changes between 48% and 97% depending on the external signal combinations. As expected, TNF is strongly apoptosis-promoting. Its effects can be significantly but incompletely offset by the external GF signal. Thus one way to investigate the irreversibility of the apoptosis process is to look at the effects of withdrawing the TNF signal after apoptosis has just started. Besides external signals, internal signals from the mitochondria component can also trigger apoptosis. Thus interrupting of this internal signal has also been considered.

Data in Table 2 suggests that apoptosis in the complete model are irreversible with respect to interruptions of either the external or the internal triggering signal. Pervious studies suggested that network irreversibility could be attributed to the presence of positive feedbacks or dual negative feedbacks (Ferrell, 2002; Ferrell and Xiong, 2001). To explore how the feedback connections in our model may affect apoptosis and its irreversibility, we compared the complete model and 15 alternative models that involve deletions of four feedback connections, either separately or in various combinations (Table 2). These include connections B and I described earlier, as well as connections A ("DNA Damage Event" to p53) and II (PTEN to PIP3). Each of connections A and B forms a positive feedback involving pro-apoptosis nodes, while each of connections I and II forms negative feedbacks involving pro-survival nodes. In what follows we will compare the complete and alternative models first in terms of the overall apoptotic ratios

Table 1
Lethal initial states and nodes having significant bias on p(ON).

Model	Apop%		Key nodes of lethal initial states (p(ON))	
	No signal	GF only	Pro-apoptosis	Pro-survival
Original	48%	47%	TNFR1 (0.54), TRADD (0.54), FADD (0.53), Cas8 (0.54), IkB (0.58), A20 (0.52), Cas3 (0.61), Cas6 (0.58), BID (0.57), p53 (0.52), Mito (0.65)[a]	IKK (0.44), NFkB (0.42), BclX (0.41), IAP (0.24)
Knockout B	22%	22%	TNFR1 (0.58), TRADD (0.65), FADD (0.64), Cas8 (0.65), IkB (0.55), APC (0.57), Cas3 (0.70), Cas6 (0.70), BID (0.55), p53 (0.53), Mito (0.66)	cFLIP (0.44), IKK (0.46), NFkB (0.43), BclX (0.44), IAP (0.13)
Knockout I	18%	15%	TRADD (0.54), Cas8 (0.54), IkB (0.66), A20 (0.58), JNK (0.59), Cas3 (0.58), Cas6 (0.56), BID (0.62), BAD (0.58), p53 (0.56), Mito (0.79)	RIP (0.46), cFLIP (0.46), TRAF2 (0.43), IKK (0.34), BclX (0.30), IAP (0.18), PIP2 (0.46), PIP3 (0.36), AKT (0.43), Mdm2 (0.42)

[a] Nodes with underline had larger than 0.6 or smaller than 0.4 p(ON).

Table 2
Apoptosis ratios (%) obtained in normal, TNF signal-interrupted and mitochondrial signal-interrupted simulations.

Model	Apop% (Ori/iTNF/iMitochrondria)			
	No signal[a]	GF only	TNF only	Double signals
Original	48/–/48[b]	47/–/47	97/97/97	64/64/64
A[c]	48/–/48	47/–/47	97/97/97	62/62/62
B	22/–/22	22/–/22	97/97/97	58/58/58
I	18/–/8	15/–/0	97/80/68	54/29/0
II	47/–/47	47/–/47	97/97/97	60/60/60
AB	22/–/22	22/–/22	97/97/97	55/55/55
AI	15/–/8	0/–/0	97/75/68	0/0/0
AII	47/–/47	47/–/47	97/97/97	59/59/59
BI	8/–/2	7/–/0	97/83/77	49/24/0
BII	22/–/22	22/–/22	97/97/97	53/53/53
I II	17/–/7	13/–/0	97/78/64	15/15/0
ABI	6/–/3	0/–/0	97/81/77	0/0/0
ABII	22/–/22	22/–/22	97/97/97	51/51/51
AI II	13/–/7	0/–/0	97/71/64	0/0/0
BI II	7/–/2	7/–/0	97/81/74	12/12/0
ALL	5/–/2	0/–/0	97/78/74	0/0/0

[a] Different input signal conditions are considered.
[b] The first number corresponds to apoptosis ratio in normal, the second in TNF signal-interrupted and the third in mitochondrial signal-interrupted simulations.
[c] 16 alternative models designed by knocking out different combinations of connections A, B, I and II labeled in Fig. 1 were considered. The letters in this column means the feedbacks that the model lost.

without signal interruptions, and then in terms of the irreversibility with respect to signal interruptions.

3.2.1. Overall apoptotic ratios

Effects of knockouts on the overall apoptotic ratio have been observed for three combinations of input signals (No signal, GF only and Double signals, respectively. See Table 2). The various knockouts have little effect on Apop% (97%) with the TNF signal ON and the GF signal OFF.

Deletions of different connections have significantly different effects on the overall apoptotic ratio. Removing one or both of the connections B (Cas6→Cas3, activating) and I (Cas3+Cas6→IAP, inhibiting) induces noticeable decreases in Apop% (from 47–48% to 15–22% without TNF signal and from 64% to 54–58% with double signals). Removing one or both of the connections A (DNA Damage Event→p53, activating) and II (PTEN→PIP3, inhibiting) has little or minor effects as long as connection I has not been removed. However, after connection I has been deleted, further deletion of either connection A or II significantly reduces Apop% (to 0–17%) at the presence of the GF signal (the only GF and double signal cases in Table 2). These results imply that the feedbacks involving connections B and I play more essential roles in promoting apoptosis than feedbacks involving connections A and II. On the other hand, at the presence of external anti-apoptotic signals such as GF, the presence of feedbacks involving A or II can partly compensate for the loss of the feedback involving I.

In our model, connections B and I are involved in positive feedbacks containing caspase 3. They are shown to play essential roles in maintaining a high Apop% without TNF. Connections A and II are related to p53. It has been suggested that positive feedbacks involving caspase 3 are responsible for the fast switching behavior of caspase 3 in apoptosis (Choi et al., 2007). Overexpression of IAPs may disrupt apoptosis (Conte et al., 2001). The small effect of deleting connection II alone is consistent with the experimental results that the inhibition of PTEN was not required for survival of some cells (Kandasamy and Srivastava, 2002; Nielsen-Preiss et al., 2003).

3.2.2. Irreversibility of apoptosis

Interestingly, among the various alternative models, only those involving the knockout of connection I showed noticeable degradations in the irreversibility of the apoptosis process (Table 2). This is true for both the TNF-interrupting and mitochondria interrupting simulations. The importance of connection I in apoptosis irreversibility agree with the ODE-based study of Legwie and Bluthgen (Legewie et al., 2006), which suggested that irreversibility of the caspase cascade might rely on significant competitive binding of activated caspases with XIAP.

Table 2 also shows that the effects of knocking out connection I are noticeably stronger when the mitochondria signal is interrupted than when the TNF signal is withdrawn. For example, in Model-I in which only connection I is missing, none of the apoptosis runs are irreversible with respect to the interruption of the mitochondria signal (interrupted Apop% = 0), but part of the runs are still irreversible with respect to the withdrawing of the TNF signal (interrupted Apop% = 29%). This result suggests that in certain cellular contexts, the apoptosis process may be associated with different degrees of irreversibility with respect to the withdrawing of extra-cellular or intra-cellular triggering signals. The disappearing of intrinsic pro-apoptotic signals may more likely lead to the abolishment of apoptosis.

Besides connection I, connection A also plays a role in irreversibility. Although knocking out connection A alone do not have much effects, alternative models missing both I and A showed significant loss of irreversibility with respect to the withdrawing of the external TNF signal as compared with those only missing connection I.

3.3. Surviving ending states and their stability

For simulations that did not end in apoptosis, the final states belong to a small set of steady surviving states. There are in total 40 such states associated with different combinations of input signals. Different surviving ending states are outcomes of varying numbers of initial states. We define the number of initial states leading to a particular ending state as the accessibility of the ending state. For a given combination of input signals, a relative accessibility for a particular ending state is defined as the fraction of initial states leading to it among all initial states that end in survival. Table 3 lists all the surviving ending states, the respective signal combinations, and the absolute and relative accessibilities.

Each of the surviving ending states has been subjected to single-node perturbations (37 perturbations for each ending state) as well as dual-node perturbations (666 perturbations in total for each ending state). Simulations starting from these perturbed states ended either in a surviving state or in apoptosis. We note the latter as survival to apoptosis (S→A) transitions. For each surviving ending state, Table 3 lists all the single-node perturbations that lead to S→A transition as well as the number of dual-node perturbations leading to the same transition. To facilitate our discussions, we group the 40 surviving ending states into four categories based on the respective number of dual-node perturbations that lead to apoptosis: "very stable" for 0, "stable" for 1–10, "unstable" for 11–100, and "very unstable" for >100. Fig. 2 represents the final states of individual nodes in each surviving ending state, ending states belonging to different categories of stability depicted with different symbols.

3.3.1. The effects of the external GF signal on stability of the surviving ending states

Table 3 suggests that although the GF signal does not significantly increase the overall survival ratio when there is no TNF signal (Table 2), the presence of the GF signal can greatly

Table 3
Surviving states and results of node-reversing experiments.

Survival states	Single reversion	Dual reversion	Signal state	Amount	Accessibility (%)
[a]0000000000010000000000000000001000000000	None	14[b]	No signal	3974	76.5[c]
0000000000010000000000000000010000000000	1, 2, 3, 7, 21, 22, 23[d]	229	No signal	578	11.1
0000000000010000000000000000000000000000	1, 2, 3, 7, 21, 22, 23	183	No signal	641	12.3
0000000000000010000000001000001111111001	None	0	GF only	521	9.9
0000000000111100000000001000001111111001	None	0	GF only	572	10.9
0000000000001000000000000000001111111001	None	0	GF only	477	9.1
0000000000101000000000000000001111111001	None	0	GF only	636	12.1
0000000000101100000000001000001111111001	None	0	GF only	716	13.6
0000000000110000000000000000001111111001	None	1	GF only	323	6.2
0000000000001100000000001000001111111001	None	0	GF only	613	11.7
0000000000100000000000000000001111111001	None	0	GF only	716	13.6
0000000000111000000000001000001111111001	None	0	GF only	357	6.8
0000000000010000000000000000001111111001	None	4	GF only	144	2.7
0000000000010100000000001000001111111001	None	4	GF only	176	3.4
1111110100010011100000000000010000000010	1, 2, 4, 6, 7, 18, 21, 22, 23	281	TNF only	79	28.3
1111110100010011100000000010010000000010	1, 2, 4, 6, 7, 18, 19, 21, 22, 23	304	TNF only	77	27.6
1111110100010011100000010101110000001010	1, 2, 4, 6, 7, 20, 21, 22, 23	284	TNF only	40	14.3
1111110100010011100000010111110000001010	1, 2, 4, 6, 7, 19, 20, 21, 22, 23	307	TNF only	83	29.7
1111111100000110000000001000001111111011	None	9	Double Signals	379	10.5
1111111100111110000000001000001111111011	None	6	Double signals	512	14.2
1111111100001010000000000000001111111011	None	6	Double signals	353	9.8
1111111100101010000000000000001111111011	None	7	Double signals	506	14.1
1111110100101100000000001000001111111011	None	0	Double signals	35	1.0
1111111100100010000000000000001111111011	30	35	Double signals	583	16.2
1111110100001010000000000000001111111011	None	0	Double signals	71	2.0
1111111100101110000000001000001111111011	None	4	Double signals	408	11.3
1111111100010010000000000000001111111011	24, 27, 30, 31	122	Double signals	58	1.6
1111110100000110000000001000001111111011	None	0	Double signals	54	1.5
1111111100110010000000000000001111111011	24, 30, 31	92	Double signals	243	6.7
1111111100011110000000001000001111111011	None	9	double signals	130	3.6
1111111100010110000000001000001111111011	30, 31	66	Double signals	30	0.8
1111110100111110000000001000001111111011	None	0	Double signals	40	1.1
1111111100001110000000001000001111111011	None	4	Double signals	120	3.3
1111110100110010000000000000001111111011	None	12	Double signals	15	0.4
1111110100001110000000001000001111111011	None	0	double signals	11	0.3
1111110100011110000000001000001111111011	None	0	Double Signals	4	0.1
1111110100010110000000001000001111111011	None	11	Double Signals	16	0.4
1111110100101010000000000000001111111011	None	0	Double signals	9	0.2
1111110100100010000000000000001111111011	None	4	Double signals	16	0.4
1111110100010010000000000000001111111011	None	18	Double signals	8	0.2

[a] State vectors of surviving states. Each bit represents a node. The highest bit represents the first node (node 1 in Fig. 1) and the lowest represents the last (node 40 in Fig. 1). The values represent the state of nodes, 0 for OFF and 1 for ON.
[b] Numbers of pairs of nodes whose reversions resulted in survival→apoptosis transitions in duel reversion experiment.
[c] For a given combination of input signals, a relative accessibility for a particular ending state is defined as the fraction of initial states leading to it among all initial states that end in survival (amount/total * 100%).
[d] Each number is a node-ID labeled in Fig. 1.

increase the stability of the final surviving states in this case. Without the GF signal, two of the three surviving ending states are not stable upon single-node perturbations. Their total relatively accessibility is 23.4%. Regarding dual node perturbations, the same two ending states are in the "very unstable" category while the remaining one is in the "unstable" category. In contrast, when the GF signal is ON, none of the surviving ending states is unstable upon single node perturbations. Upon dual-node perturbations, majority of the surviving ending states are in the "very stable" category and the remaining three (with a total relative accessibility of 12.3%) in the "stable" category.

At the presence of the TNF signal and when the GF signal is OFF, all of the surviving ending states are not stable upon some single-node perturbations, and belong to the "very unstable" category upon dual-node perturbations. When the GF signal is also ON, not only the survival ratio increases (Table 2), the stability of the surviving states also increases significantly (Table 3). The total relative accessibility of stable surviving ending states upon single-node perturbations is 74.6%. Upon dual-node perturbations, most of the respective surviving states belong to the "very stable" or "stable" categories. Only one state (with an accessibility of 1.6%) belongs to the "very unstable" category.

3.3.2. Nodes promoting survival to apoptosis transitions in single-node perturbations

The single-node perturbations listed in Table 3 suggest that fluctuations in the states of those nodes in the GF and NFκB signaling pathways in general do not result in S→A transitions in all four combinations of external signals. Fluctuations in the states of the nodes in the TNF signal pathway (TNFR1, TRADD, TRAF, cFLIP and Cas8) and all nodes in the caspase cascade result in S→A transitions mostly when there is no GF signal. Fluctuations of the four intrinsic nodes, p53, IAP, Mito and Bid, on the other hand, may result in S→A transitions mostly when there is GF signal.

3.3.3. Nodes playing some controlling roles in the stability of the surviving ending states at different input combinations

Fig. 2 suggests that there are some important correlations between the stability of the surviving ending states and the state of individual nodes in those states.

Without any external signals, there are three surviving ending states, one with IAP ON and the other two with IAP OFF (Fig. 2a). The state with IAP ON is stable upon single-node perturbation and is associated with only14 dual-node perturbations that lead to S→A transitions. The other two states are much less stable upon either type of perturbations. In contrast to IAP, the activation of mitochondria exhibits strong destabilizing effects. Of the three surviving ending states, the one with Mito activated is the most unstable one (Table 3).

With only the TNF signal ON, the only 4 surviving states are all very unstable. The IAP node is OFF and the mitochondria node is ON in all of them (Fig. 2b). These states are "survival" only because Cas8 was inhibited by cFLIP before the activation of the downstream pro-apoptotic pathways.

With only the GF signal ON, all 11 surviving states belong to either the "stable" or "very stable" category. Comparisons of the states of individual nodes imply the importance of NFκB: the states with NFκB ON and IkB OFF are more stable (Fig. 2c).

With both TNF and GF signals ON, NFκB and Cas8 exhibited dominant effects. States with NFκB ON and Cas8 OFF all belong to the "very stable" category, while states with NFκB OFF and Cas8 ON all belong to either the "unstable" or "very unstable" categories (Fig. 2d). It is interesting to note that IAP is always in the activated state in these surviving ending states, but states with activated IAP can still be unstable.

The above results may be correlated with reported levels of expression of IAP, NFκB and caspase-8 in tumor cells. Such cells may be associated with high stability of the surviving states. IAP was reported to have a high level of expression in different cells (Endo et al., 2004; Hofmann et al., 2002; Nemoto et al., 2004). However, from its expression level alone one could not individually predict the effects of chemotherapy in non-small-cell lung cancer (NSCLC) (Ferreira et al., 2001). NFκB has different levels of expression in NSCLC cells and the apoptotic rate was lower in cells with higher NFκB expressions (Zhang et al., 2006). Caspase-8 was up-regulated in NSCLC cells in the pro-caspase form. The apoptotic rate was significantly higher in the cells with a stronger immunostaining pattern of caspase-8 (Tormanen-Napankangas et al., 2001).

4. Conclusions

In summary, we have analyzed the apoptosis network using a Boolean model. Based on simulations started from randomly

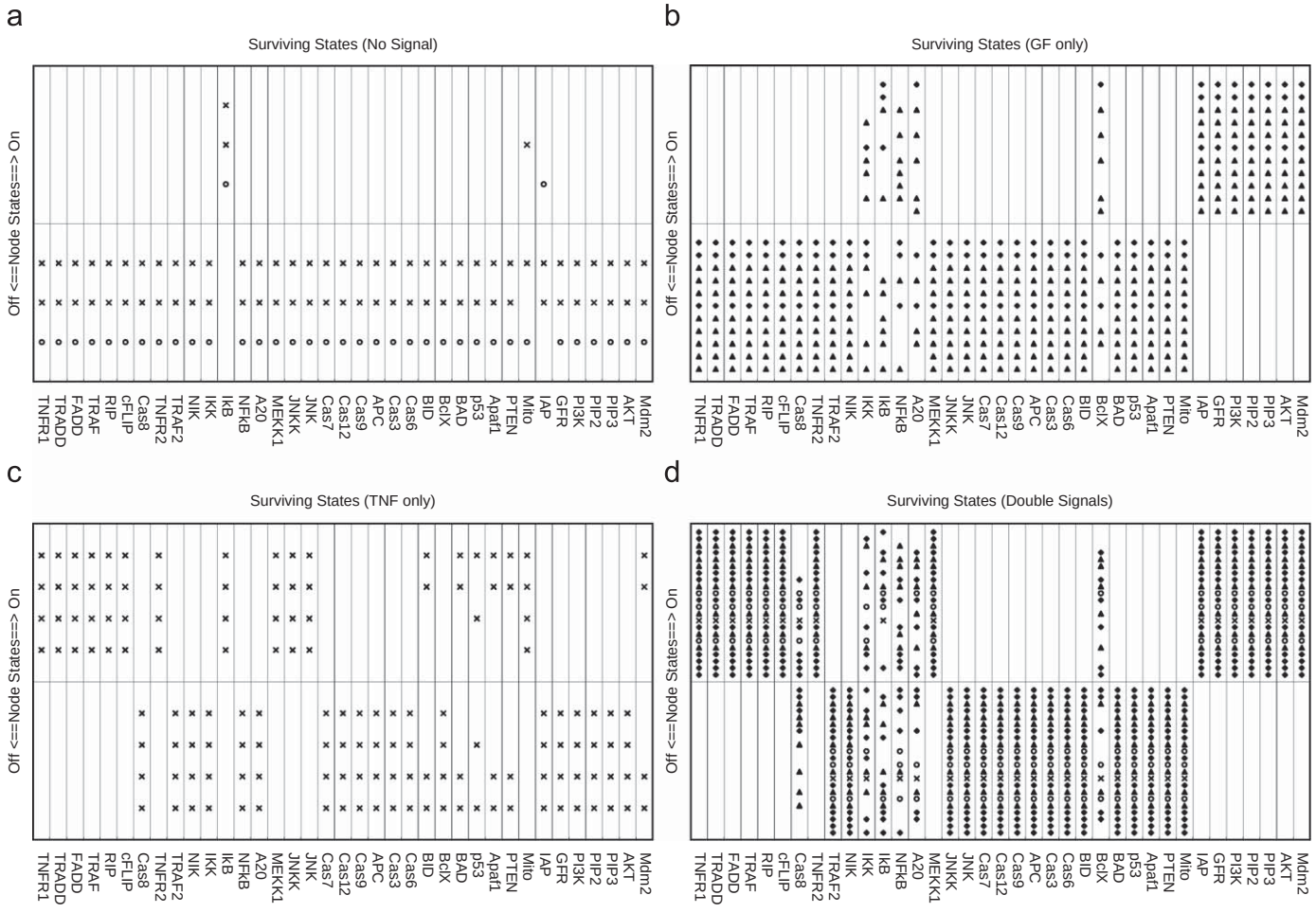

Fig. 2. States of individual nodes in and the stability category of different surviving states. Each node corresponds to one column. Each surviving state corresponds to two lines of symbols, one above zero and another below zero. A symbol in a column and a line above (below) zero indicates that the corresponding node in a particular survival state is in the ON (OFF) state. The shapes of the symbols represent stability categories of surviving states: solid triangles for "very stable", solid diamonds for "stable", circles for "unstable" and crosses for "very unstable". Steady surviving states under different input signal conditions are shown: (a) no signal; (b) TNF only; (c) GF only; and (d) GF and TNF.

sampled initial states, the model is able to reproduce well-known pro-apoptotic and pro-survival molecular components (nodes). The effects of the initial states of some but not all of these nodes depend on the presence/missing of certain key feedback loops. The model suggested that although irreversibility of the apoptosis process indeed depends on the presence of feedback loops in the network structure, not all the four feedback loops investigated in this work contributed similarly. Two of the investigated feedbacks directly involving Cas3 are essential in promoting apoptosis as well as in maintaining its irreversibility. The other two feedbacks related to p53 showed compensating effects only when the former two are missing. Moreover, disruptions in the intrinsic pro-apoptotic signal are more likely to induce abolishment of apoptosis than the withdrawing of the extra-cellular signal. These were found to be consistent with previous experimental or in silico results (Conte et al., 2001; Legewie et al., 2006). We found that the external GF signal was of key importance for the stability of the surviving states of the network. The states of a few key nodes in surviving states are also strongly correlated to the stability of the respective network state.

The above results suggested some general design principles of the apoptosis network. The irreversibility of the apoptosis process and the stability of the surviving states might, at first sight, be mutually exclusive. The apoptosis network seems to have achieved both in the same network framework by using different components to control the two properties. The irreversibility of apoptosis mostly and redundantly relies on down-stream positive feedback loops, while the stability of the surviving states depends more on the presence of external pro-survival signals. Such a design may provide some plasticity for cell apoptosis to adapt to different biological contexts. The strength of the external pro-survival signal may control how easy or difficult it can be to trigger apoptosis, but once the cell enters apoptosis, the process cannot be reversed.

Our model necessarily involves large simplifications: components are represented only as nodes with two possible states; dynamics are governed by simple rules replacing complex molecular processes. However, using such a simplified model allowed us to model a more complete network than using ODE models involving detailed dynamics. The network model has included known molecular pathways integrating external and intrinsic apoptotic and surviving signals. Given the simplifications and the lack of detailed knowledge about the status of various cellular components under many experimental circumstances, we did not try to approximate experimental results obtained in a particular cellular context. Instead, we performed simulations starting from randomly initial states with unbiased distributions, and extracted and analyzed systems properties based on statistics. It is important to note that many of the computer generated initial states cannot be realized in real experiments (e.g., the cell cannot survive), but they do contain valuable information for the characterization and understanding of the design principles of the network.

Compared with ODE models, Boolean networks are certainly limited in approximating experimental results and in making context-specific quantitative predictions of cellular dynamics. Our work suggested that BN models, however, might allow for easier integration of various experimental information and more systematic explorations in both the model space and state space, and provide results that are readily subjected to a variety of statistical analyses. As interest in systems level properties and how such properties emerge from the integration of various network components increases, we expect that BN models like those presented here will complements other types of in silico approaches as well as experimental ones in studies of complex cellular networks.

Acknowledgments

This work has been supported by the Chinese Natural Science Foundation (Grant no. 90403120) and the Chinese Ministry of Science and Technology (Grant nos. 2006AA02Z303 and 2006CB910700).

Appendix A. Supplementary material

Supplementary data associated with this article can be found in the online version at doi:10.1016/j.jtbi.2009.04.024.

References

Albeck, J.G., Burke, J.M., et al., 2008. Quantitative analysis of pathways controlling extrinsic apoptosis in single cells. Mol. Cell 30, 11–25.
Amaral, L.A.N., Diaz-Guilera, A., et al., 2004. Emergence of complex dynamics in a simple model of signaling networks. Proc. Natl. Acad. Sci. USA 101, 15551–15555.
Bagci, E.Z., Vodovotz, Y., et al., 2006. Bistability in apoptosis: roles of bax, bcl-2, and mitochondrial permeability transition pores. Biophys. J. 90, 1546–1559.
Bentele, M., Lavrik, I., et al., 2004. Mathematical modeling reveals threshold mechanism in CD95-induced apoptosis. J. Cell Biol. 166, 839–851.
Bernal-Mizrachi, L., Lovly, C.M., et al., 2006. The role of NF-{kappa}B-1 and NF-{kappa}B-2-mediated resistance to apoptosis in lymphomas. Proc. Natl. Acad. Sci. USA 103, 9220–9225.
Budihardjo, I., Oliver, H., et al., 1999. Biochemical pathways of caspase activation during apoptosis. Annu. Rev. Cell Dev. Biol. 15, 269–290.
Choi, H.S., Han, S., et al., 2007. Coupled positive feedbacks provoke slow induction plus fast switching in apoptosis. FEBS Lett. 581, 2684–2690.
Conte, D., Liston, P., et al., 2001. Thymocyte-targeted overexpression of xiap transgene disrupts T lymphoid apoptosis and maturation. Proc. Natl. Acad. Sci. USA 98, 5049–5054.
De Valck, D., Heyninck, K., et al., 1997. A20 inhibits NF-kappaB activation independently of binding to 14-3-3 proteins. Biochem. Biophys. Res. Commun. 238, 590–594.
Deveraux, Q.L., Reed, J.C., 1999. IAP family proteins—suppressors of apoptosis. Genes Dev. 13, 239–252.
Deveraux, Q.L., Takahashi, R., et al., 1997. X-linked IAP is a direct inhibitor of cell-death proteases. Nature 388, 300–304.
Eissing, T., Conzelmann, H., et al., 2004. Bistability analyses of a caspase activation model for receptor-induced apoptosis. J. Biol. Chem. 279, 36892–36897.
Endo, T., Abe, S., et al., 2004. Expression of IAP family proteins in colon cancers from patients with different age groups. Cancer Immunol. Immunother. 53, 770–776.
Falschlehner, C., Emmerich, C.H., et al., 2007. TRAIL signalling: decisions between life and death. Int. J. Biochem. Cell Biol. 39, 1462–1475.
Ferran, C., Stroka, D.M., et al., 1998. A20 inhibits NF-kappaB activation in endothelial cells without sensitizing to tumor necrosis factor-mediated apoptosis. Blood 91, 2249–2258.
Ferreira, C.G., van der Valk, P., et al., 2001. Assessment of IAP (inhibitor of apoptosis) proteins as predictors of response to chemotherapy in advanced non-small-cell lung cancer patients. Ann. Oncol. 12, 799–805.
Ferrell Jr, J.E., 2002. Self-perpetuating states in signal transduction: positive feedback, double-negative feedback and bistability. Curr. Opin. Cell Biol. 14, 140–148.
Ferrell, J.E., Xiong, W., 2001. Bistability in cell signaling: how to make continuous processes discontinuous, and reversible processes irreversible. Chaos 11, 227–236.
Gross, A., McDonnell, J.M., et al., 1999. BCL-2 family members and the mitochondria in apoptosis. Genes Dev. 13, 1899–1911.
Haupt, S., Berger, M., et al., 2003. Apoptosis—the p53 network. J. Cell Sci. 116, 4077–4085.
Henson, E.S., Gibson, S.B., 2006. Surviving cell death through epidermal growth factor (EGF) signal transduction pathways: implications for cancer therapy. Cell Signal. 18, 2089–2097.
Hofmann, H.S., Simm, A., et al., 2002. Expression of inhibitors of apoptosis (IAP) proteins in non-small cell human lung cancer. J. Cancer Res. Clin. Oncol. 128, 554–560.
Huang, S., Ingber, D.E., 2000. Shape-dependent control of cell growth, differentiation, and apoptosis: switching between attractors in cell regulatory networks. Exp. Cell Res. 261, 91–103.
Janes, K.A., Albeck, J.G., et al., 2005. A systems model of signaling identifies a molecular basis set for cytokine-induced apoptosis. Science 310, 1646–1653.
Kandasamy, K., Srivastava, R.K., 2002. Role of the phosphatidylinositol 3′-kinase/PTEN/Akt kinase pathway in tumor necrosis factor-related apoptosis-inducing ligand-induced apoptosis in non-small cell lung cancer cells. Cancer Res. 62, 4929–4937.

Kauffman, S., 1969. Metabolic stability and epigenesis in randomly constructed genetic nets. Theor. Biol. 22, 437–467.
Kelliher, M.A., Grimm, S., et al., 1998. The death domain kinase RIP mediates the TNF-induced NF-kappaB signal. Immunity 8, 297–303.
Kim, W.H., Lee, J.W., et al., 2005. Synergistic activation of JNK/SAPK induced by TNF-alpha and IFN-gamma: apoptosis of pancreatic beta-cells via the p53 and ROS pathway. Cell Signal. 17, 1516–1532.
Ko, C.H., Shen, S.C., et al., 2005. Mitochondrial-dependent, reactive oxygen species-independent apoptosis by myricetin: roles of protein kinase C, cytochrome c, and caspase cascade. Biochem. Pharmacol. 69, 913–927.
Legewie, S., Bluthgen, N., et al., 2006. Mathematical modeling identifies inhibitors of apoptosis as mediators of positive feedback and bistability. PLoS Comput. Biol. 2, e120.
Li, F., Long, T., et al., 2004. The yeast cell-cycle network is robustly designed. Proc. Natl. Acad. Sci. USA 101, 4781–4786.
Li, Y., Mao, Y., et al., 2005. Selective induction of apoptosis through the FADD/caspase-8 pathway by a p53 c-terminal peptide in human pre-malignant and malignant cells. Int. J. Cancer 115, 55–64.
Lin, Y., Devin, A., et al., 2000. The death domain kinase RIP is essential for TRAIL (Apo2L)-induced activation of IkappaB kinase and c-Jun N-terminal kinase. Mol. Cell Biol. 20, 6638–6645.
Lowe, S.W., Cepero, E., et al., 2004. Intrinsic tumour suppression. Nature 432, 307–315.
Mak, T.W., Yeh, W.C., 2002. Signaling for survival and apoptosis in the immune system. Arthritis Res. 4 (3), S243–S252.
Morgan, M.J., Thorburn, J., et al., 2001. An apoptosis signaling pathway induced by the death domain of FADD selectively kills normal but not cancerous prostate epithelial cells. Cell Death Differ. 8, 696–705.
Muppidi, J.R., Tschopp, J., et al., 2004. Life and death decisions: secondary complexes and lipid rafts in TNF receptor family signal transduction. Immunity 21, 461–465.
Narita, M., Shimizu, S., et al., 1998. Bax interacts with the permeability transition pore to induce permeability transition and cytochrome c release in isolated mitochondria. Proc. Natl. Acad. Sci. USA 95, 14681–14686.
Nemoto, T., Kitagawa, M., et al., 2004. Expression of IAP family proteins in esophageal cancer. Exp. Mol. Pathol. 76, 253–259.
Nielsen-Preiss, S.M., Silva, S.R., et al., 2003. Role of PTEN and Akt in the regulation of growth and apoptosis in human osteoblastic cells. J. Cell Biochem. 90, 964–975.
Okamura, A., Iwata, N., et al., 2006. Casein kinase Iepsilon down-regulates phospho-Akt via PTEN, following genotoxic stress-induced apoptosis in hematopoietic cells. Life Sci. 78, 1624–1629.
Philchenkov, A., 2004. Caspases: potential targets for regulating cell death. J. Cell Mol. Med. 8, 432–444.
Rehm, M., Huber, H.J., et al., 2006. Systems analysis of effector caspase activation and its control by X-linked inhibitor of apoptosis protein. Embo J. 25, 4338–4349.
Sartorius, U., Schmitz, I., et al., 2001. Molecular mechanisms of death-receptor-mediated apoptosis. Chem. Biochem. 2, 20–29.
Shimizu, S., Narita, M., et al., 1999. Bcl-2 family proteins regulate the release of apoptogenic cytochrome c by the mitochondrial channel VDAC. Nature 399, 483–487.
Shu, H.B., Takeuchi, M., et al., 1996. The tumor necrosis factor receptor 2 signal transducers TRAF2 and c-IAP1 are components of the tumor necrosis factor receptor 1 signaling complex. Proc. Natl. Acad. Sci. USA 93, 13973–13978.
Song, G., Ouyang, G., et al., 2005. The activation of Akt/PKB signaling pathway and cell survival. J. Cell Mol. Med. 9, 59–71.
Stelling, J., 2004. Mathematical models in microbial systems biology. Curr. Opin. Microbiol. 7, 513–518.
Tormanen-Napankangas, U., Soini, Y., et al., 2001. Expression of caspases-3, -6 and -8 and their relation to apoptosis in non-small cell lung carcinoma. Int. J. Cancer 93, 192–198.
Wang, E., Marcotte, R., et al., 1999. Signaling pathway for apoptosis: a racetrack for life or death. J. Cell Biochem. 32–33 (Suppl), 95–102.
Wolkenhauer, O., 2002. Mathematical modelling in the post-genome era: understanding genome expression and regulation—a system theoretic approach. Biosystems 65, 1–18.
Wu, C.J., Conze, D.B., et al., 2005. TNF-alpha induced c-IAP1/TRAF2 complex translocation to a Ubc6-containing compartment and TRAF2 ubiquitination. Embo J. 24, 1886–1898.
Yan, X., Fraser, M., et al., 2006. Over-expression of PTEN sensitizes human ovarian cancer cells to cisplatin-induced apoptosis in a p53-dependent manner. Gynecol. Oncol. 102, 348–355.
Yu, J., Zhang, L., 2005. The transcriptional targets of p53 in apoptosis control. Biochem. Biophys. Res. Commun. 331, 851–858.
Zhang, Z., Ma, J., et al., 2006. Expression of nuclear factor-kappaB and its clinical significance in nonsmall-cell lung cancer. Ann. Thorac. Surg. 82, 243–248.